Inhibition of Plasmepsin V Activity Blocks Plasmodium falciparum Gametocytogenesis and Transmission to Mosquitoes

Author

Jennison, Charlie, Lucantoni, Leonardo, O'Neill, Matthew T, McConville, Robyn, Erickson, Sara M, Cowman, Alan F, Sleebs, Brad E, Avery, Vicky M, Boddey, Justin A

Published

2019

Journal Title

Cell Reports

Version

Version of Record (VoR)

DOI

10.1016/j.celrep.2019.11.073

Report

Cell Reports

Inhibition of Plasmepsin V Activity Blocks *Plasmodium falciparum* Gametocytogenesis and Transmission to Mosquitoes

Graphical Abstract

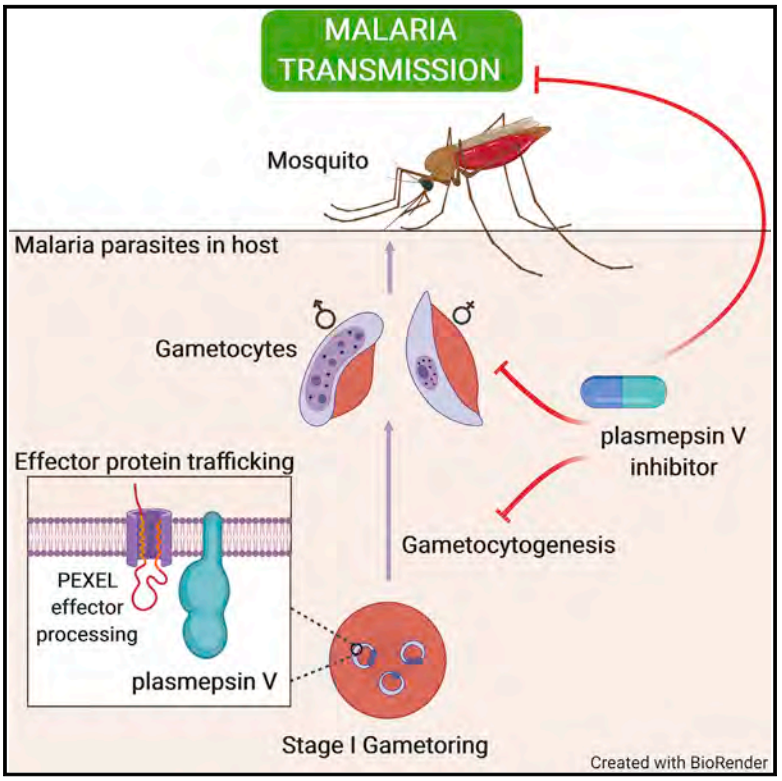

Authors

Charlie Jennison, Leonardo Lucantoni, Matthew T. O'Neill, ..., Brad E. Sleebs, Vicky M. Avery, Justin A. Boddey

Correspondence

boddey@wehi.edu.au

In Brief

Plasmodium falciparum gametocytes infect mosquitoes and are responsible for malaria transmission. Jennison et al. discover that the aspartyl protease plasmepsin V is essential for *P. falciparum* gametocyte development. The inhibition of plasmepsin V prevents *P. falciparum* infection of mosquitoes, validating this enzyme as a transmission-blocking drug target.

Highlights

- Plasmepsin V is expressed and can be inhibited in *P. falciparum* gametocytes
- Plasmepsin V inhibition disrupts export of gametocyte proteins and gametocytogenesis
- Plasmepsin V inhibition blocks *P. falciparum* infection of *Anopheles* mosquitoes

Jennison et al., 2019, Cell Reports *29*, 3796–3806
December 17, 2019
https://doi.org/10.1016/j.celrep.2019.11.073

CellPress

OPEN ACCESS
CellPress

Cell Reports
Report

Inhibition of Plasmepsin V Activity Blocks *Plasmodium falciparum* Gametocytogenesis and Transmission to Mosquitoes

Charlie Jennison,[1,2] Leonardo Lucantoni,[3] Matthew T. O'Neill,[1] Robyn McConville,[1,2] Sara M. Erickson,[1,2] Alan F. Cowman,[1,2] Brad E. Sleebs,[1,2] Vicky M. Avery,[3] and Justin A. Boddey[1,2,4,*]
[1]The Walter and Eliza Hall Institute of Medical Research, Parkville 3052, VIC, Australia
[2]Department of Medical Biology, University of Melbourne, Parkville 3010, VIC, Australia
[3]Discovery Biology, Griffith Institute for Drug Discovery, Griffith University, Nathan 4111, QLD, Australia
[4]Lead Contact
*Correspondence: boddey@wehi.edu.au
https://doi.org/10.1016/j.celrep.2019.11.073

SUMMARY

Plasmodium falciparum **gametocytes infect mosquitoes and are responsible for malaria transmission. New interventions that block transmission could accelerate malaria elimination. Gametocytes develop within erythrocytes and activate protein export pathways that remodel the host cell. Plasmepsin V (PMV) is an aspartyl protease that is required for protein export in asexual parasites, but its function and essentiality in gametocytes has not been definitively proven, nor has PMV been assessed as a transmission-blocking drug target. Here, we show that PMV is expressed and can be inhibited specifically in *P. falciparum* stage I-II gametocytes. PMV inhibitors block processing and export of gametocyte effector proteins and inhibit development of stage II-V gametocytes. Gametocytogenesis in the presence of sublethal inhibitor concentrations results in stage V gametocytes that fail to infect mosquitoes. Therefore, PMV primes gametocyte effectors for export, which is essential for the development and fitness of gametocytes for transmission to mosquitoes.**

INTRODUCTION

In 2017, *Plasmodium falciparum* caused 617,000 deaths from malaria (Weiss et al., 2019). Malaria is curable, but drug treatment failure and resistance throughout Asia (Hamilton et al., 2019; van der Pluijm et al., 2019) are some of the most dangerous risks to malaria control. Malaria is caused by *Plasmodium* parasites that are transmitted by mosquitoes. Gametocytes are the only parasite stage that can be transmitted to mosquitoes, and they are a prime life cycle target for transmission-blocking intervention (Burrows et al., 2017).

Most antimalarial drugs are not gametocytocidal (Bolscher et al., 2015; Delves et al., 2016; Lucantoni et al., 2016), rendering patients receiving many antimalarials reservoirs for transmission. Primaquine has gametocytocidal and hypnozoitocidal activity, but it is toxic in people with glucose-6-phosphate deficiency, a common trait in endemic regions (White, 2013). New gametocytocidal drugs are needed and a specific target candidate profile (TCP 5) has been developed to address this unmet need (Burrows et al., 2017). An important drug development milestone is identifying suitable targets. *P. falciparum* gametocytes undertake 5 stages of development lasting 10–12 days (Hawking et al., 1971). Gametocyte physiology changes through development, rendering mature forms insensitive to many drugs that kill asexual parasites (Srivastava et al., 2016). The efficacy of gametocytocidal compounds also varies between male and female gametocytes (Chotivanich et al., 2006; Delves et al., 2018; Ruecker et al., 2014). It has been suggested that gametocytogenesis may be a transmission-blocking target that is preferable to mature gametocytes (Sinden, 2017).

Gametocyte differentiation begins when parasites sense low levels of host lysophosphatidylcholine (Brancucci et al., 2017). Transcriptional reprogramming is initiated by gametocyte development 1 (GDV1) (Eksi et al., 2012; Filarsky et al., 2018) and ApiAP2 involved in gametocytogenesis (AP2-G) (Kafsack et al., 2014; Sinha et al., 2014). Like their asexual counterparts, sexual merozoites infect erythrocytes and export effector proteins (Dantzler et al., 2019; Silvestrini et al., 2010; Tibúrcio et al., 2012). *P. falciparum* asexual parasites export >400 effectors (Sargeant et al., 2006), and so far, >60 gametocyte exported proteins (GEXPs) have been identified (Silvestrini et al., 2010). While a subset is shared with asexual stages, several are absent or unique to gametocytes (Dantzler et al., 2019; Tibúrcio et al., 2012). The varied exportomes may be associated with different parasite-host interactions, including cytoadherence of asexual parasites (reviewed by Kraemer and Smith, 2006) versus gametocyte extravasation and development in the bone marrow and spleen (De Niz et al., 2018; Joice et al., 2014; Obaldia et al., 2018) before mature gametocytes return to the circulation for transmission (Pelle et al., 2015).

Protein export involves two mechanisms (reviewed by Boddey and Cowman, 2013; Spielmann and Gilberger, 2015). The most common involves the recognition of cargo containing the *Plasmodium* export element (PEXEL) (Hiller et al., 2004; Marti et al., 2004) and translocation into the endoplasmic reticulum (ER) by a sec61 sec62 complex (Marapana et al., 2018). PEXEL processing at the leucine residue (Boddey et al.,

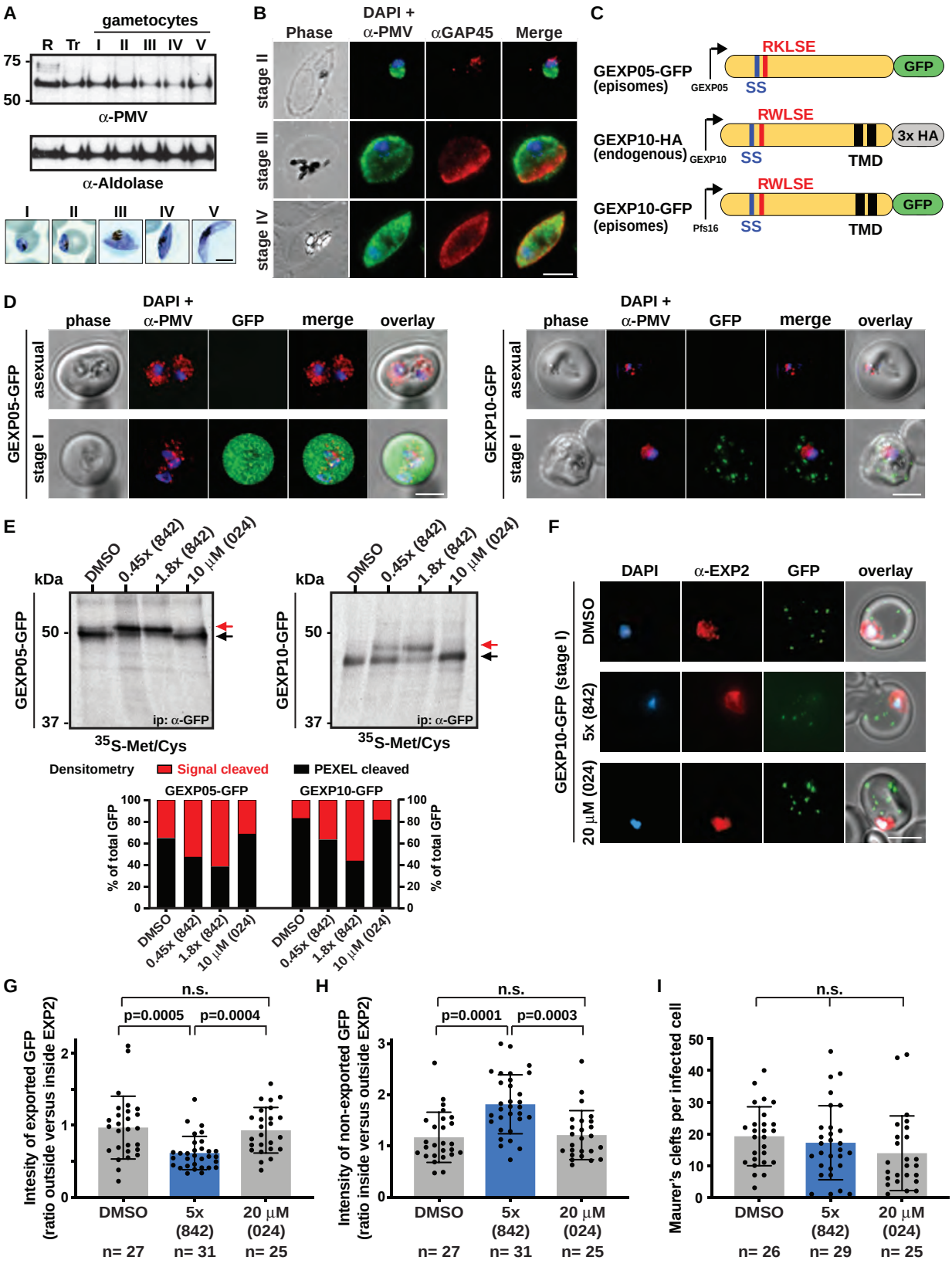

(legend on next page)

2009; Chang et al., 2008) by the aspartyl protease plasmepsin V (PMV) (Boddey et al., 2010; Russo et al., 2010) primes them for export. PEXEL-cleaved proteins are translocated into the host cell via the *Plasmodium* translocon of exported proteins (PTEX) (Beck et al., 2014; de Koning-Ward et al., 2009; Elsworth et al., 2014; Ho et al., 2018). PEXEL proteins, PMV and PTEX are essential in asexual parasites (Beck et al., 2014; Boddey et al., 2010; Elsworth et al., 2014; Garten et al., 2018; Maier et al., 2008; Marapana et al., 2018; Russo et al., 2010; Sleebs et al., 2014a). Two PEXEL-containing proteins (Ikadai et al., 2013) and the PTEX component HSP101 (Beck et al., 2014) are essential in early gametocytes, but PMV has not been studied in sexual stages.

PMV can be inhibited with compounds that mimic the transition state of PEXEL cleavage (Gambini et al., 2015; Gazdik et al., 2015, 2016; Hodder et al., 2015; Sleebs et al., 2014a, 2014b). PMV inhibitors WEHI-916, WEHI-842, and WEHI-601 kill *P. falciparum* asexual parasites by inhibiting the processing and export of PEXEL proteins (Hodder et al., 2015; Nguyen et al., 2018; Sleebs et al., 2014a). Riboswitch-dependent knockdown (Prommana et al., 2013) of PMV sensitized parasites to inhibitors, and the expression of extra copies caused modest resistance, providing evidence that PMV was the target (Sleebs et al., 2014a). Analogs WEHI-024 and WEHI-025 that mimic non-cleavable PEXEL mutant substrates have minimal activity against PMV or *P. falciparum* (Sleebs et al., 2014a). These compounds provide an opportunity to study PMV across the life cycle.

Here, we investigated the function, essentiality, and transmission-blocking potential of PMV in gametocytes using inhibitors. We show that PMV is active, primes GEXPs for export, can be inhibited, and is essential in *P. falciparum* gametocytes and for transmission to mosquitoes.

RESULTS

PMV Is Expressed and Can Be Inhibited Specifically in Gametocytes

To determine whether PMV is expressed in gametocytes, we performed immunoblotting and microscopy with specific antibodies. PMV was expressed in each stage of gametocytogenesis (Figure 1A) and was localized around the nucleus in stage I-II gametocytes (Figures 1B and 1D), similar to asexual parasites, indicating that it was within the ER (Klemba and Goldberg, 2005). In stage III, the inner membrane complex (IMC) is produced, involving the transport of components from the ER to the IMC. IMC growth coincides with the augmentation of the ER around the stage III parasite, which no longer forms a perinuclear structure (Dearnley et al., 2012). In agreement with this description, we observed PMV in the perinuclear ER in close proximity to the IMC component glideosome-associated protein 45 (GAP45) (Baum et al., 2006) in stage II gametocytes followed by augmentation of the PMV signal around the cell in stages III-IV, which coincides with GAP45 incorporation into the IMC (Figure 1B). Therefore, PMV is expressed in the perinuclear ER in stage I-II gametocytes, and its dynamic localization in stage III-IV is consistent with previously described morphological changes during gametocytogenesis (Dearnley et al., 2012).

To investigate PMV function in gametocytes, we chose two PEXEL proteins for further study, GEXP05 and GEXP10 (Silvestrini et al., 2010). We used *P. falciparum* parasites in which GEXP05 fused to GFP was expressed from its native gametocyte-specific promoter (Tibúrcio et al., 2015) (Figure 1C). For GEXP10, an Hyp8 family protein (Sargeant et al., 2006; Sleebs et al., 2014a), we generated *P. falciparum* parasites that expressed GEXP10-HA (hemagglutinin tag) from the native locus (Figure 1C). While GEXP10 is expressed in gametocytes, we

Figure 1. PMV Expression and Inhibition in *P. falciparum* Gametocytes

(A) PMV expression in asexual rings (R), asexual trophozoites (Tr), and gametocytes at stage I (day 2), stage II (day 4), stage III (day 6), stage IV (day 9), and stage V (day 12) by immunoblot with rabbit anti-PMV antibodies. Aldolase was a loading control. Giemsa-stained gametocyte stages are shown. Scale bar, 5 μm.

(B) Immunofluorescence microscopy with mouse anti-PMV and rabbit anti-GAP45 antibodies show expression at the perinuclear ER in stage II gametocytes. The ER including PMV is redistributed around the cell, and GAP45 is incorporated into the IMC in stage III-IV gametocytes as described (Dearnley et al., 2012). Scale bar, 5 μm.

(C) Schematic of GEXP05 and GEXP10 proteins used in this study. PEXEL is in red. HA, hemagglutinin tag; SS, signal sequence; TMD, transmembrane domain.

(D) GEXP05-GFP and GEXP10-GFP are not expressed in asexual parasites, but they are expressed and exported in stage I gametocytes. Rabbit anti-PMV antibodies show expression at the perinuclear ER in asexual and sexual stages. Scale bar, 5 μm.

(E) ^{35}S-Methionine labeling and immunoprecipitation (IP) with anti-GFP antibodies of GEXP05-GFP and GEXP10-GFP in stage II gametocytes (day 3). PEXEL-cleaved species are indicated (black arrow). Pre-incubation with WEHI-842 for 3 h at 0.45× (2.5 μM) and 1.8× (10 μM) EC_{50} reduced PEXEL cleavage and caused the accumulation of larger signal peptide-cleaved species (red arrow). WEHI-024 (10 μM) had no effect. Densitometry of bands in each lane is shown below.

(F) Maximum intensity projections of stage I gametocytes (20 h post-invasion) showing EXP2 at the parasitophorous vacuole membrane and export of GEXP10-GFP to MCs. Cells were prepared by allowing sexual merozoites to invade for 15 min; 16 h later they were treated with drugs for 4 h (WEHI-842, 5× EC_{50}, 20 μM; WEHI-024 control, 20 μM), fixed, and imaged. Scale bar, 5 μm.

(G) Quantification of GEXP10-GFP export by stage I gametocytes, for which an example was shown in (F). Total GFP pixel intensity was measured outside the EXP2 signal within the erythrocyte (in MCs; exported) and also inside the EXP2 signal (non-exported). The intensity of exported GFP is shown as a ratio outside to inside EXP2, as described previously (Sleebs et al., 2014a). Data are a single representative from 3 independent experiments (see Figure S2 for data).

(H) Quantification of non-exported GEXP10-GFP by stage I gametocytes using the same micrographs as (G). The intensity of non-exported GFP is shown as a ratio inside to outside EXP2. WEHI-842 caused the accumulation of GEXP10-GFP in the parasite. Data are a single representative from 3 independent experiments (see Figure S2 for data).

(I) Number of MCs per gametocyte-infected erythrocyte (GFP^+ puncta outside the EXP2 signal), quantified using the same micrographs as (G). WEHI-842 did not reduce the MC number per cell, as some processing and export of GEXP10-GFP occurred. Data are a single representative from 2 independent experiments (see Figure S2 for data).

Data in (G)–(I) are means ± SDs. Comparisons were performed using the Kruskal-Wallis test (Dunn's multiple comparisons). The number (n) of gametocyte-infected erythrocytes counted is shown. WEHI-842 concentrations are a function of the EC_{50} (see Figure 2D). $p < 0.05$ is statistically significant; n.s., not significant.

observed GEXP10-HA expression in asexual rings and trophozoites, where it was exported and co-localized with skeleton-binding protein 1 (SBP1) (Figures S1A and S1B). Immunoelectron microscopy showed localization in Maurer's clefts (MCs) (Figure S1A). Detergent solubilization and trypsin digestion revealed the topology of GEXP10, such that the N and C termini were facing the erythrocyte cytosol (Figure S1C). Given the possibility that GEXP10 may facilitate the trafficking of erythrocyte membrane protein 1 (PfEMP1) (Maier et al., 2008), we produced genetically disrupted parasites by inserting a cassette into the *GEXP10* gene (Figures S1D and S1E). This did not affect the export of other parasite proteins to MCs, knobs, erythrocyte cytoskeleton, or PfEMP1 display on the erythrocyte surface (Figures S1F and S1G). Therefore, GEXP10 is an exported protein that is not essential for growth or assembly of the cytoadherence complex in asexual stages. The mutant was generated in strain CS2 to study PfEMP1 (Var2CSA) trafficking (Maier et al., 2008). However, CS2 did not produce gametocytes, and the characterization of sexual stages was not possible.

To study GEXP10 specifically in gametocytes, we expressed it under the control of a stage-specific promoter to distinguish sexual from asexual stages. As CS2 does not produce gametocytes, we used strain NF54 to generate parasites in which GEXP10-GFP was expressed from the gametocyte-specific *Pfs16* promoter (Figure 1C). Immunofluorescence microscopy confirmed that GEXP10-GFP was not expressed in asexual stages, but was exported to punctate structures that are consistent with MCs in early gametocytes (Figure 1D).

PMV activity in gametocytes was then examined by radiolabeling proteins for 10 min before immunoprecipitating GEXP05-GFP and GEXP10-GFP, visualizing bands by autoradiography, and quantifying them by densitometry. Radiolabeled GEXP05-GFP and GEXP10-GFP were present as a major species, with sizes corresponding to the predicted PEXEL-cleaved proteins (Figure 1E). The addition of PEXEL-mimetic compound WEHI-842, which potently inhibits PEXEL cleavage by PMV in *P. falciparum* asexual stages (Hodder et al., 2015), to gametocytes for 3 h before radiolabeling caused a dose-dependent accumulation of larger GEXP05-GFP and GEXP10-GFP species, which is consistent with the predicted signal peptide-cleaved proteins (Figure 1E). Densitometry showed WEHI-842 reduced PEXEL cleavage by >50% (at 1.8× half-maximal effective concentration [EC_{50}]) and increased the amount of the larger species in gametocytes. However, WEHI-024 that mimics a non-cleavable PEXEL substrate and does not inhibit PMV in asexual stages (Sleebs et al., 2014a) had no effect (Figure 1E). These results are similar to the inhibition of PEXEL cleavage by WEHI-842 in asexual stages (Hodder et al., 2015), indicating that PMV is active and can be inhibited specifically in gametocytes.

To determine whether PMV activity is required for protein export in gametocytes, we treated them with inhibitors and used microscopy to quantify the amount of GEXP10-GFP exported beyond the EXP2-labeled parasitophorous vacuole (PV) membrane into the host cell (Figure 1F). The addition of WEHI-842 to synchronous 16-h-old gametorings, when the *Pfs16* promoter had activated, for 4 h reduced the amount of exported GFP in the host cell (outside EXP2) by ~50% compared to DMSO and WEHI-024 controls ($p = 0.0005$; Figures 1G and S2). Concomitantly, WEHI-842 increased the amount of non-exported GFP (retained inside the EXP2 signal) compared to controls ($p = 0.0003$; Figures 1H and S2). This was similar to the effects caused by PMV inhibitors on export in asexual stages (Sleebs et al., 2014a). No difference in the number of MCs per gametocyte-infected cell ($GEXP10^+$ GFP puncta) was observed (Figure 1I), indicating that export was not completely inhibited at the concentrations used (Sleebs et al., 2014a). These results show that cleavage and export of GEXPs could be inhibited by PMV inhibitors.

PMV Inhibitors Have Gametocytocidal Activity

To determine whether PMV is essential in gametocytes, $NF54^{Pfs16}$ that expresses GFP-luciferase from the *Pfs16* promoter (Adjalley et al., 2011) was differentiated into sexual stages, treated with inhibitors (Figure 2A), and luciferase expression measured to determine gametocyte viability (Lucantoni et al., 2013). PMV inhibitors WEHI-842 or WEHI-916 (Hodder et al., 2015; Sleebs et al., 2014a) were added to gametocyte-committed schizonts for 48 h to ensure exposure to gametorings following egress. The inhibitors killed gametocytes with a half-maximal effective concentration (EC_{50}) of 1.55 (±0.11) and of 9.03 (±0.34) μM, respectively (Figure 2B). The potency shift between compounds was similar to that reported in asexual stages (Hodder et al., 2015). Using an imaging-based assay (Duffy and Avery, 2012), the baseline activity of WEHI-842 and WEHI-916 against asexual stages was 1.58 (±0.16) and 7.63 (±0.24) μM (strain 3D7) and 1.63 (±0.09) and 9.76 (±0.65) μM (strain D10), respectively. Control analogs WEHI-024 and WEHI-025, which are poorly active against PMV (Sleebs et al., 2014a), had a negligible effect on gametocyte development (Figure 2B). Control compounds artesunate, amodiaquine, chloroquine, and tafenoquine were included to validate the assay (Lucantoni et al., 2013), and gametocyte death occurred as expected.

To determine the stage of gametocytogenesis that PMV was essential, inhibitors were added to gametocyte cultures at later times (Figure 2A). WEHI-842 and WEHI-916 potency decreased against successively later sexual stages (Figures 2C and 2D). Analogs WEHI-024 and WEHI-025 were inactive against all of the gametocyte stages tested, while artesunate and tafenoquine killed all of the stages and chloroquine and amodiaquine inhibited early stages only, as expected (Figure 2D).

PMV Inhibitors Prevent Development of Stage II-V Gametocytes

To identify when PMV inhibitors cause arrest, we performed microscopy of blood smears and quantified gametocyte stages (Hliscs et al., 2015). In agreement with the luciferase assay, daily dosing of WEHI-842 starting at early stage I (Figure 3A) caused a rapid decline in gametocytemia (Figure 3B). The majority of parasites that received 1.25× EC_{50} concentration were deformed or pyknotic by day 3 and no stage II-V gametocytes were seen (Figures 3C and 3D). As the parasites did not recover from this treatment, the majority with this appearance were dying or dead. A reduced concentration (0.5× EC_{50}) permitted a small number of stage III parasites to develop, but few stage IV-V parasites were seen thereafter (Figures 3C and 3D). A concentration of 0.25× EC_{50} resulted in successful development to stage V

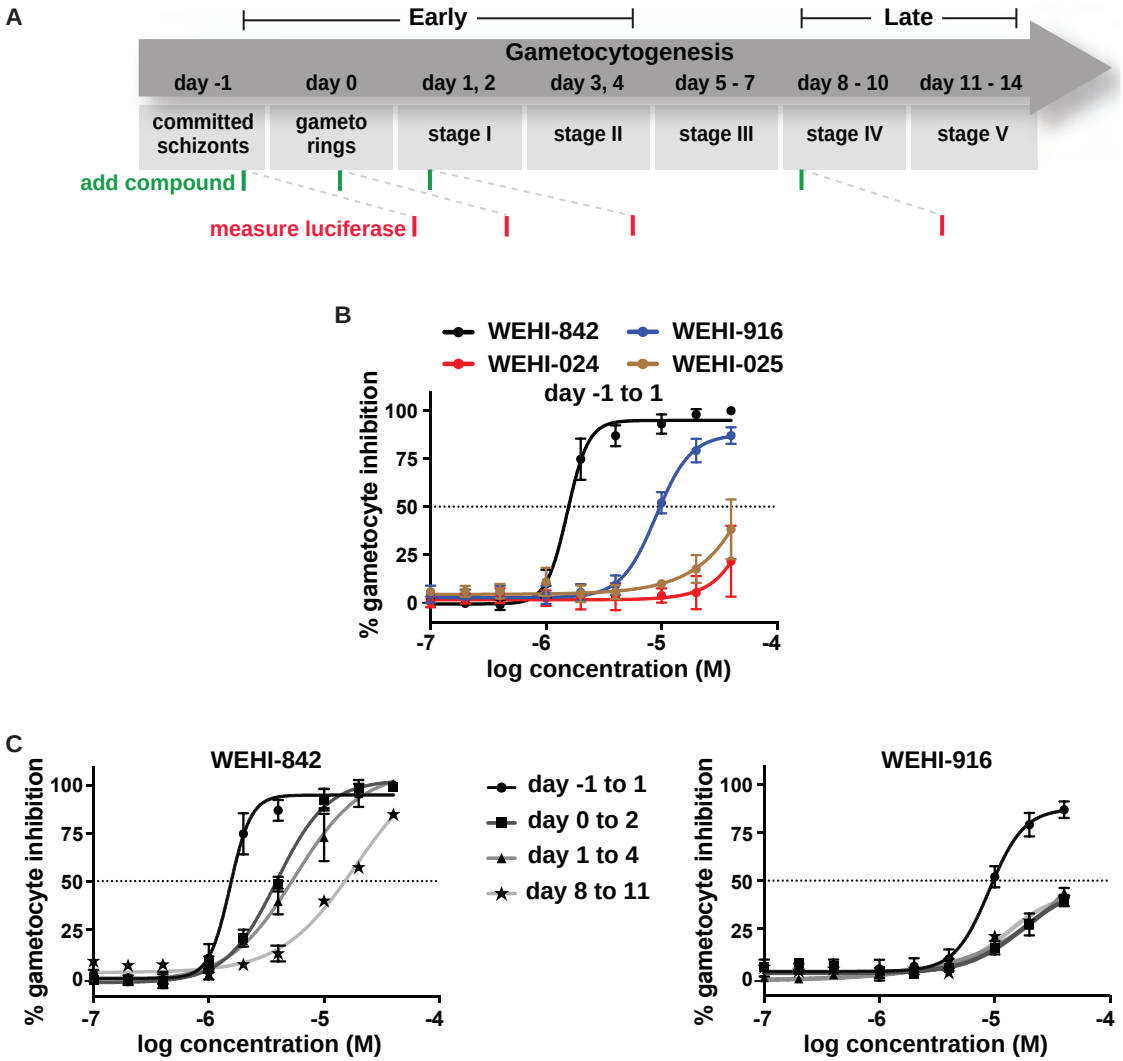

D

	day -1 to 1	day 0 to 2	day 1 to 4	day 8 to 11
	EC_{50} (SEM) (nM)	EC_{50} (SEM) (nM)	EC_{50} (SEM) (nM)	EC_{50} (SEM) (nM)
WEHI-842	1579 (159)	3914 (40)	5619 (417)	~15300*
WEHI-916	7629 (237)	Not converged	Not converged	Not converged
WEHI-024	>100000	Not converged	Not converged	Not converged
WEHI-025	>100000	Not converged	Not converged	Not converged
tafenoquine	2498 (690)	885 (301)	2684 (306)	17095 (2559)
chloroquine	20.4 (5.3)	16.3 (0.9)	172 (6)	inactive
amodiaquine	9 (3)	7 (0.2)	219 (5)	inactive
artesunate	3(2)	2 (0.7)	32 (0.6)	23 (2)

Figure 2. PMV Inhibitors Have Gametocytocidal Activity

(A) Schematic of the different stages of gametocytogenesis in which inhibitors were tested.

(B) Dose-response curves of *P. falciparum* NF54^{Pfs16} in the presence of PMV inhibitors and analog controls, day −1 to 1.

(C) Dose-response curves of *P. falciparum* NF54^{Pfs16} in the presence of inhibitors at different days of gametocytogenesis.

(D) Summary of gametocytocidal activity of PMV inhibitors and control drugs. Not converged indicates <50% inhibition at the maximum concentration of 40 μM.

*EC_{50} could not be accurately determined due to the lack of a full inhibition plateau in curve (85% ± 1% inhibition at 40 μM).

Data in (B) and (C) are means ± SDs and in (D) are means ± SEMs, from n = 3 independent experiments.

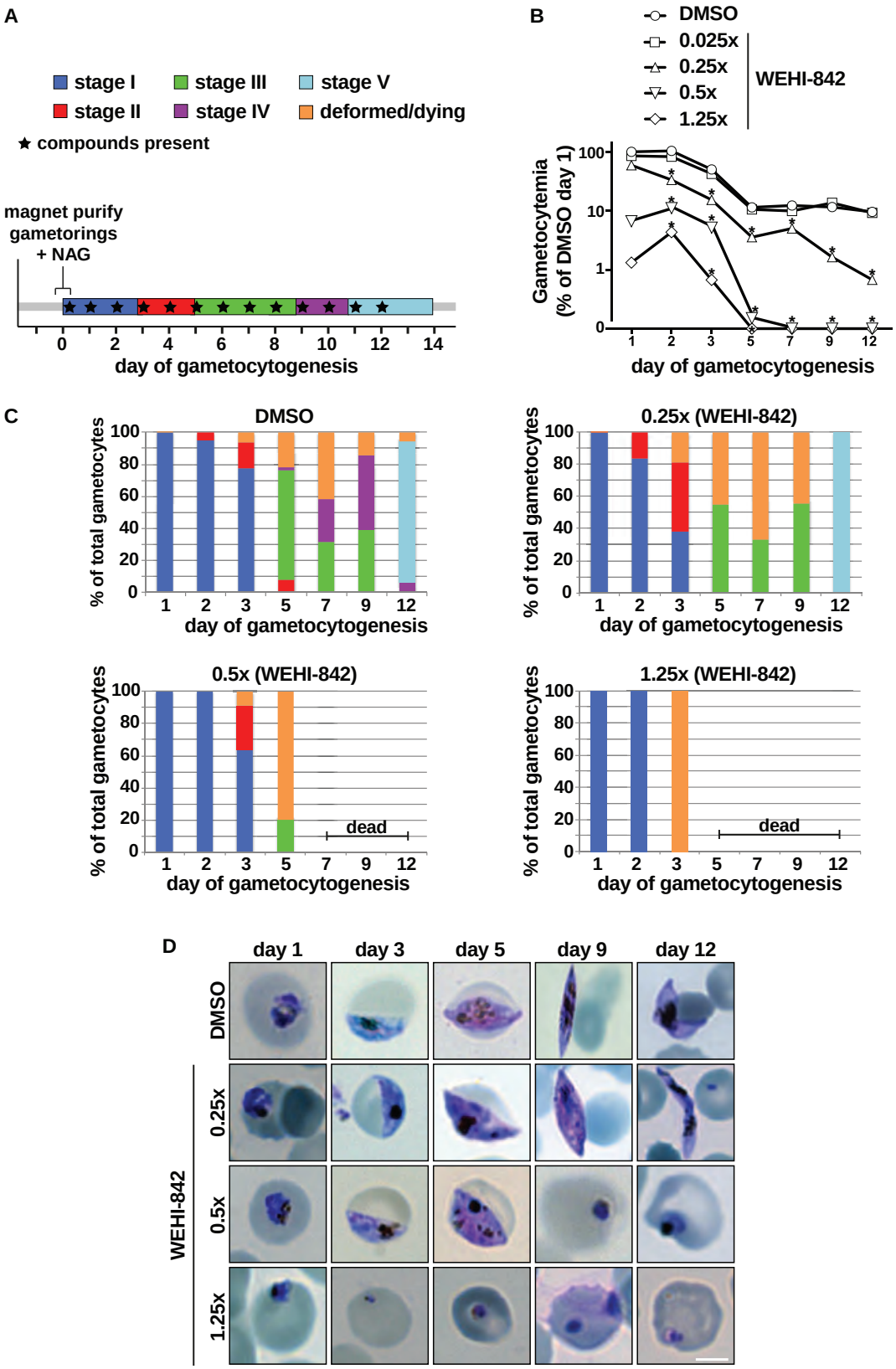

(legend on next page)

(Figures 3C and 3D), although gametocytemia was less than with DMSO (Figure 3B). Sublethal WEHI-842 concentrations permitted development to stage V, although whether the parasites were transmissible remained to be tested. This showed that PMV inhibitors attenuate gametocyte development at stage I, in agreement with protein export occurring at this stage (Dantzler et al., 2019; Silvestrini et al., 2010).

PMV Is Required for Transmission to Mosquitoes

We next determined whether gametocytes treated with PMV inhibitors were infectious to mosquitoes. Magnet purification during commitment (Figure 3A) resulted in poor transmission of subsequent stage V gametocytes (results not shown), so we used the standard "crash method" of gametocyte differentiation (Saliba and Jacobs-Lorena, 2013), dosing PMV inhibitors using two treatment regimens (Figure 4A). Treatment 1 involved adding drugs to stage I gametocytes for 7 days followed by culture in drug-free media and transmitting parasites to mosquitoes by standard membrane feeding assays (SMFAs). Treatment 2 involved adding drugs at stage V on the day of mosquito feeding to assess downstream steps in infection. One week post-SMFA, mosquito midguts were dissected, and oocyst intensity and infection prevalence were enumerated.

With treatment 1, WEHI-842 had a dose-dependent inhibitory effect on gametocyte development, oocyst intensity, and infection prevalence, while controls had no effect (Figures 4B, 4C, and S3). The lowest dose of 0.25× EC_{50} WEHI-842 permitted the development of stage V gametocytes; however, these were attenuated for mosquito infection, indicating that they had reduced transmission fitness. Conversely with treatment 2, WEHI-842 had no effect (Figure 4D). This suggests that PMV inhibitors do not affect gamete egress, fertilization, or ookinete infectivity. The results show that PMV inhibitors attenuate gametocyte development and fitness, but not gamete fertilization or ookinete formation leading to oocyst development.

DISCUSSION

The *Plasmodium* life cycle can be interrupted at several stages, and blocking gametocyte transmission to the mosquito is a prime example (Blagborough et al., 2013). Several lines of evidence suggest that the protein export pathway may be a suitable target in gametocytes for blocking transmission. First, PMV and PTEX are expressed in gametocytes (Florens et al., 2002; Silvestrini et al., 2010). Second, many PEXEL effector proteins are expressed in gametocytes (Dantzler et al., 2019; Silvestrini et al., 2010; Tibúrcio et al., 2015). Third, the genetic disruption of two genes encoding PEXEL proteins arrests gametocytogenesis at stage I (Ikadai et al., 2013). Fourth, conditional knockdown of PTEX (HSP101) inhibited gametocytogenesis at stage I (Beck et al., 2014). Lastly, PEXEL-cleaved and *N*-acetylated peptides were detected by mass spectrometry of gametocytes, suggesting that PMV was active (Silvestrini et al., 2010).

Here, we used inhibitors that block PEXEL processing, export, and *P. falciparum* asexual growth (Hodder et al., 2015; Sleebs et al., 2014a) to characterize PMV in gametocytes. In asexual stages, PMV knockdown with *glmS* sensitized parasites to inhibitors, demonstrating that it was a direct target (Sleebs et al., 2014a). We were unable to achieve knockdown in gametocytes due to poor conversion rates in the presence of the *glmS* inducer glucosamine. While we cannot exclude the possibility that our compounds hit another protease(s), they disrupted PEXEL processing, export, and gametocyte development, with efficacy peaking against stage I, the time that gametocytes export proteins (Silvestrini et al., 2010), which is consistent with the inhibition of PMV. The gametocyte phenotypes were similar to those reported for asexual stages, where PMV inhibitors added to rings killed them, preventing the development of trophozoites (Hodder et al., 2015; Sleebs et al., 2014a). In addition, analogs that mimic non-cleavable PEXEL substrates, which have little inhibitory activity against PMV (Sleebs et al., 2014a), had no effect on PEXEL cleavage, export, gametocyte development, or transmission in this study. These results point to PMV being essential in both asexual and sexual stages due to the need for PEXEL processing for export. *Plasmodium* effectors have various functions, including trafficking of other proteins and virulence factors through and onto the surface of the erythrocyte (Maier et al., 2008) and activating new permeability pathways in the erythrocyte membrane (Gero and Wood, 1991; Staines et al., 2000), allowing the transport of solutes (Kirk and Lehane, 2014). The *P. falciparum* exportome comprises >400 proteins (Sargeant et al., 2006), and identifying which are essential in asexual and sexual stages remains to be elucidated.

We successfully generated GEXP10 mutant parasites. GEXP10 was not required for the asexual growth or export of proteins to MCs, erythrocyte cytoskeleton, and knobs, nor was it involved in PfEMP1 trafficking (Maier et al., 2008). These phenotypes fit with GEXP10 expression also in gametocytes, which do not express knobs or PfEMP1 (Tibúrcio et al., 2012). We localized GEXP10 to MCs in asexual and sexual parasites. GEXP10 also localizes to the infected erythrocyte surface (Dantzler et al., 2019; Hermand et al., 2016). MCs are involved in trafficking proteins to the cell surface (reviewed in Boddey and Cowman, 2013), and we may have localized GEXP10 in transit to the surface. Our results that the GEXP10 N and C termini face the erythrocyte cytosol accommodates both MC and surface localization, in which the loop between transmembrane domains is exposed to the MC lumen

Figure 3. PMV Inhibitors Block Development of Stage II-V Gametocytes

(A) Schematic of *P. falciparum* NF54 gametocyte induction, their stages (colors as indicated), and drug treatment used.

(B) Gametocytemia after drug treatment determined by counting Giemsa-stained blood smears (relative to DMSO on day 1). WEHI-842 concentrations were 0.1, 1, 2, and 5 μM, shown as a function of EC_{50} (see Figure 2D). Gametocytemia was compared to DMSO using Fisher's exact test; significant differences are indicated above (*$p < 0.001$).

(C) Gametocyte stage distribution over time. Colors correspond to stages shown in (A).

(D) Giemsa-stained blood smears under indicated conditions. Scale bar, 5 μm.

Data are a single representative of n = 3 independent experiments.

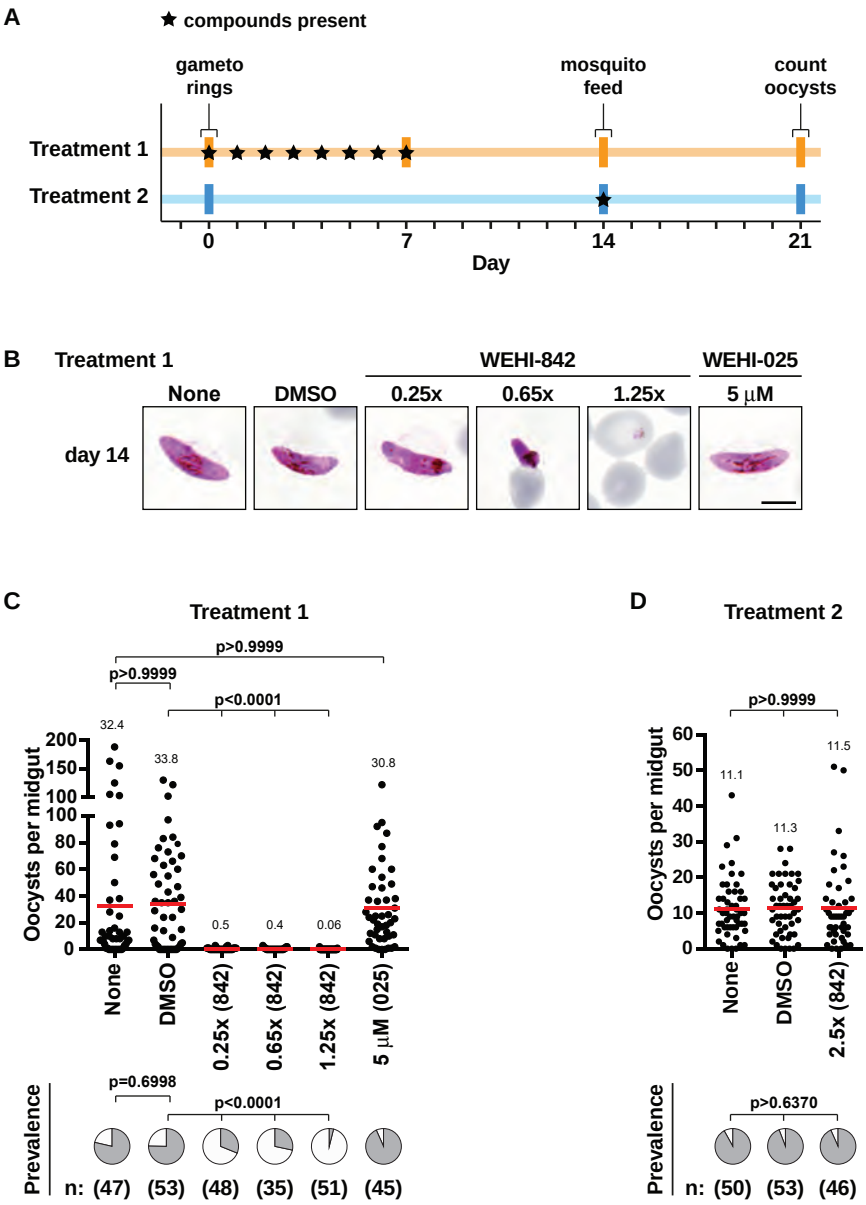

Figure 4. PMV Inhibitors Block Transmission to Mosquitoes

(A) Schematic of *P. falciparum* NF54 gametocyte induction and drug treatments used. Media was changed once daily; parasites were not washed.

(B) Giemsa-stained blood smears on the day of mosquito feeding. WEHI-842 concentrations were 1, 2.5, and 5 μM, shown as a function of EC_{50} (see Figure 2D). WEHI-025 at 5 μM was equal to highest WEHI-842 concentration used. Scale bar, 5 μm.

(C) Mosquito oocyst intensity (top) and infection prevalence (bottom) following Treatment 1, as shown in (A).

(D) Mosquito oocyst intensity (top) and infection prevalence (bottom) following Treatment 2, as shown in (A).

(C and D) Mean oocyst number is indicated above each condition and with a red bar within each condition. Mosquito sample size (n) is shown. Oocysts were compared using Kruskal-Wallis test with Dunn's correction and prevalence compared using the chi-square test. Data are a single representative from 3 independent replicates (see Figure S3 for data). $p < 0.05$ is statistically significant.

or the erythrocyte surface following translocation to the membrane. This is consistent with studies detecting GEXP10 on the surface using antibodies raised to the loop (Dantzler et al., 2019; Hermand et al., 2016). As the GEXP10 mutant did not produce gametocytes, its function in such stages remains to be elucidated.

Gametocytogenesis may be an attractive transmission-blocking target for malaria (Sinden, 2017). Our study shows that PMV inhibitors block gametocytogenesis, but they do not affect gametes or ookinete infection. That WEHI-842 had transmission-blocking activity at sublethal concentrations at which stage V gametocytes formed suggests that even partial inhibition of PMV affects transmission fitness. Combined with previous studies that elucidated the essentiality of PMV in asexual stages (Boddey et al., 2010; Boonyalai et al., 2018; Hodder et al., 2015; Russo et al., 2010; Sleebs et al., 2014a), this study validates PMV as a dual life cycle stage antimalarial drug target.

STAR★METHODS

Detailed methods are provided in the online version of this paper and include the following:

- KEY RESOURCES TABLE
- LEAD CONTACT AND MATERIALS AVAILABILITY
- EXPERIMENTAL MODEL AND SUBJECT DETAILS
  - Culture Conditions for Parasite Maintenance
  - *P. falciparum* Gametocyte EC_{50} Determination
  - Inhibition of Gametocyte Development

SUPPLEMENTAL INFORMATION

Supplemental Information can be found online at https://doi.org/10.1016/j.celrep.2019.11.073.

ACKNOWLEDGMENTS

We thank the Australian Red Cross for the erythrocytes; Sash Lopaticki, Svenja Gunther, Annie Yang, Michelle Gazdik, and Lachlan Whitehead for technical assistance; and Matthew Dixon and Pietro Alano for the GEXP05-GFP parasites. This work was supported by NHMRC project grants (1010326 and 1049811), the Cass Foundation (Science and Medicine Grant SM/6430), Victorian State Government Operational Infrastructure Support, and Australian Government NHMRC IRIISS. A.F.C. is a Howard Hughes International Scholar, B.E.S. is an Ellen Corin Centenary Fellow, and J.A.B. is an NHMRC R.D. Wright Fellow.

AUTHOR CONTRIBUTIONS

J.A.B. and A.F.C. conceived and designed experiments; C.J., L.L., M.T.O., R.M., S.M.E., and J.A.B. performed the experiments; C.J., L.L., M.T.O., B.E.S., A.F.C., V.M.A., and J.A.B. analyzed the data; and all authors contributed to writing the paper.

DECLARATION OF INTERESTS

A.F.C., B.E.S., and J.A.B. are inventors on patent WO/2016/19719, "Structure of Plasmepsin V in Complex with an Inhibitor and Uses Thereof."

Received: July 29, 2019
Revised: October 14, 2019
Accepted: November 15, 2019
Published: December 17, 2019

REFERENCES

Adjalley, S.H., Johnston, G.L., Li, T., Eastman, R.T., Ekland, E.H., Eappen, A.G., Richman, A., Sim, B.K., Lee, M.C., Hoffman, S.L., and Fidock, D.A. (2011). Quantitative assessment of *Plasmodium falciparum* sexual development reveals potent transmission-blocking activity by methylene blue. Proc. Natl. Acad. Sci. USA *108*, E1214–E1223.

Anderluh, G., Pungercar, J., Strukelj, B., Macek, P., and Gubensek, F. (1996). Cloning, sequencing, and expression of equinatoxin II. Biochem. Biophys. Res. Commun. *220*, 437–442.

Armistead, J.S., Jennison, C., O'Neill, M.T., Lopaticki, S., Liehl, P., Hanson, K.K., Annoura, T., Rajasekaran, P., Erickson, S.M., Tonkin, C.J., et al. (2018). *Plasmodium falciparum* subtilisin-like ookinete protein SOPT plays an important and conserved role during ookinete infection of the Anopheles stephensi midgut. Mol. Microbiol. *109*, 458–473.

Bahl, A., Brunk, B., Coppel, R.L., Crabtree, J., Diskin, S.J., Fraunholz, M.J., Grant, G.R., Gupta, D., Huestis, R.L., Kissinger, J.C., et al. (2002). PlasmoDB: the *Plasmodium* genome resource. An integrated database providing tools for accessing, analyzing and mapping expression and sequence data (both finished and unfinished). Nucleic Acids Res. *30*, 87–90.

Baum, J., Richard, D., Healer, J., Rug, M., Krnajski, Z., Gilberger, T.W., Green, J.L., Holder, A.A., and Cowman, A.F. (2006). A conserved molecular motor drives cell invasion and gliding motility across malaria life cycle stages and other apicomplexan parasites. J. Biol. Chem. *281*, 5197–5208.

Beck, J.R., Muralidharan, V., Oksman, A., and Goldberg, D.E. (2014). PTEX component HSP101 mediates export of diverse malaria effectors into host erythrocytes. Nature *511*, 592–595.

Blagborough, A.M., Churcher, T.S., Upton, L.M., Ghani, A.C., Gething, P.W., and Sinden, R.E. (2013). Transmission-blocking interventions eliminate malaria from laboratory populations. Nat. Commun. *4*, 1812.

Boddey, J.A., and Cowman, A.F. (2013). *Plasmodium* nesting: remaking the erythrocyte from the inside out. Annu. Rev. Microbiol. *67*, 243–269.

Boddey, J.A., Moritz, R.L., Simpson, R.J., and Cowman, A.F. (2009). Role of the *Plasmodium* export element in trafficking parasite proteins to the infected erythrocyte. Traffic *10*, 285–299.

Boddey, J.A., Hodder, A.N., Günther, S., Gilson, P.R., Patsiouras, H., Kapp, E.A., Pearce, J.A., de Koning-Ward, T.F., Simpson, R.J., Crabb, B.S., and Cowman, A.F. (2010). An aspartyl protease directs malaria effector proteins to the host cell. Nature *463*, 627–631.

Bolscher, J.M., Koolen, K.M., van Gemert, G.J., van de Vegte-Bolmer, M.G., Bousema, T., Leroy, D., Sauerwein, R.W., and Dechering, K.J. (2015). A combination of new screening assays for prioritization of transmission-blocking antimalarials reveals distinct dynamics of marketed and experimental drugs. J. Antimicrob. Chemother. *70*, 1357–1366.

Boonyalai, N., Collins, C.R., Hackett, F., Withers-Martinez, C., and Blackman, M.J. (2018). Essentiality of *Plasmodium falciparum* plasmepsin V. PLoS One *13*, e0207621.

Boyle, M.J., Wilson, D.W., Richards, J.S., Riglar, D.T., Tetteh, K.K., Conway, D.J., Ralph, S.A., Baum, J., and Beeson, J.G. (2010). Isolation of viable *Plasmodium falciparum* merozoites to define erythrocyte invasion events and advance vaccine and drug development. Proc. Natl. Acad. Sci. USA *107*, 14378–14383.

Brancucci, N.M.B., Gerdt, J.P., Wang, C., De Niz, M., Philip, N., Adapa, S.R., Zhang, M., Hitz, E., Niederwieser, I., Boltryk, S.D., et al. (2017). Lysophosphatidylcholine Regulates Sexual Stage Differentiation in the Human Malaria Parasite Plasmodium falciparum. Cell *171*, 1532–1544.e15.

Burrows, J.N., Duparc, S., Gutteridge, W.E., Hooft van Huijsduijnen, R., Kaszubska, W., Macintyre, F., Mazzuri, S., Möhrle, J.J., and Wells, T.N.C. (2017). New developments in anti-malarial target candidate and product profiles. Malar. J. *16*, 26.

Chang, H.H., Falick, A.M., Carlton, P.M., Sedat, J.W., DeRisi, J.L., and Marletta, M.A. (2008). N-terminal processing of proteins exported by malaria parasites. Mol. Biochem. Parasitol. *160*, 107–115.

Chotivanich, K., Sattabongkot, J., Udomsangpetch, R., Looareesuwan, S., Day, N.P., Coleman, R.E., and White, N.J. (2006). Transmission-blocking activities of quinine, primaquine, and artesunate. Antimicrob. Agents Chemother. *50*, 1927–1930.

Cooke, B.M., Rogerson, S.J., Brown, G.V., and Coppel, R.L. (1996). Adhesion of malaria-infected red blood cells to chondroitin sulfate A under flow conditions. Blood *88*, 4040–4044.

Dantzler, K.W., Ma, S., Ngotho, P., Stone, W.J.R., Tao, D., Rijpma, S., De Niz, M., Nilsson Bark, S.K., Jore, M.M., Raaijmakers, T.K., et al. (2019). Naturally acquired immunity against immature *Plasmodium falciparum* gametocytes. Sci. Transl. Med. *11*, eaav3963.

de Koning-Ward, T.F., Gilson, P.R., Boddey, J.A., Rug, M., Smith, B.J., Papenfuss, A.T., Sanders, P.R., Lundie, R.J., Maier, A.G., Cowman, A.F., and Crabb, B.S. (2009). A newly discovered protein export machine in malaria parasites. Nature *459*, 945–949.

De Niz, M., Meibalan, E., Mejia, P., Ma, S., Brancucci, N.M.B., Agop-Nersesian, C., Mandt, R., Ngotho, P., Hughes, K.R., Waters, A.P., et al. (2018).

Plasmodium gametocytes display homing and vascular transmigration in the host bone marrow. Sci. Adv. *4*, eaat3775.

Dearnley, M.K., Yeoman, J.A., Hanssen, E., Kenny, S., Turnbull, L., Whitchurch, C.B., Tilley, L., and Dixon, M.W. (2012). Origin, composition, organization and function of the inner membrane complex of *Plasmodium falciparum* gametocytes. J. Cell Sci. *125*, 2053–2063.

Delves, M.J., Straschil, U., Ruecker, A., Miguel-Blanco, C., Marques, S., Dufour, A.C., Baum, J., and Sinden, R.E. (2016). Routine in vitro culture of *P. falciparum* gametocytes to evaluate novel transmission-blocking interventions. Nat. Protoc. *11*, 1668–1680.

Delves, M.J., Miguel-Blanco, C., Matthews, H., Molina, I., Ruecker, A., Yahiya, S., Straschil, U., Abraham, M., León, M.L., Fischer, O.J., et al. (2018). A high throughput screen for next-generation leads targeting malaria parasite transmission. Nat. Commun. *9*, 3805.

Duffy, S., and Avery, V.M. (2012). Development and optimization of a novel 384-well anti-malarial imaging assay validated for high-throughput screening. Am. J. Trop. Med. Hyg. *86*, 84–92.

Duffy, S., and Avery, V.M. (2013). Identification of inhibitors of *Plasmodium falciparum* gametocyte development. Malar. J. *12*, 408.

Duffy, S., Loganathan, S., Holleran, J.P., and Avery, V.M. (2016). Large-scale production of *Plasmodium falciparum* gametocytes for malaria drug discovery. Nat. Protoc. *11*, 976–992.

Duraisingh, M.T., Triglia, T., and Cowman, A.F. (2002). Negative selection of *Plasmodium falciparum* reveals targeted gene deletion by double crossover recombination. Int. J. Parasitol. *32*, 81–89.

Eksi, S., Morahan, B.J., Haile, Y., Furuya, T., Jiang, H., Ali, O., Xu, H., Kiattibutr, K., Suri, A., Czesny, B., et al. (2012). *Plasmodium falciparum* gametocyte development 1 (Pfgdv1) and gametocytogenesis early gene identification and commitment to sexual development. PLoS Pathog. *8*, e1002964.

Elsworth, B., Matthews, K., Nie, C.Q., Kalanon, M., Charnaud, S.C., Sanders, P.R., Chisholm, S.A., Counihan, N.A., Shaw, P.J., Pino, P., et al. (2014). PTEX is an essential nexus for protein export in malaria parasites. Nature *511*, 587–591.

Filarsky, M., Fraschka, S.A., Niederwieser, I., Brancucci, N.M.B., Carrington, E., Carrió, E., Moes, S., Jenoe, P., Bártfai, R., and Voss, T.S. (2018). GDV1 induces sexual commitment of malaria parasites by antagonizing HP1-dependent gene silencing. Science *359*, 1259–1263.

Florens, L., Washburn, M.P., Raine, J.D., Anthony, R.M., Grainger, M., Haynes, J.D., Moch, J.K., Muster, N., Sacci, J.B., Tabb, D.L., et al. (2002). A proteomic view of the *Plasmodium falciparum* life cycle. Nature *419*, 520–526.

Gambini, L., Rizzi, L., Pedretti, A., Taglialatela-Scafati, O., Carucci, M., Pancotti, A., Galli, C., Read, M., Giurisato, E., Romeo, S., and Russo, I. (2015). Picomolar Inhibition of Plasmepsin V, an Essential Malaria Protease, Achieved Exploiting the Prime Region. PLoS One *10*, e0142509.

Garten, M., Nasamu, A.S., Niles, J.C., Zimmerberg, J., Goldberg, D.E., and Beck, J.R. (2018). EXP2 is a nutrient-permeable channel in the vacuolar membrane of *Plasmodium* and is essential for protein export via PTEX. Nat. Microbiol. *3*, 1090–1098.

Gazdik, M., O'Neill, M.T., Lopaticki, S., Lowes, K.N., Smith, B.J., Cowman, A.F., Boddey, J.A., and Sleebs, B.E. (2015). The effect of N-methylation on transition state mimetic inhibitors of the *Plasmodium* protease, plasmepsin V. MedChemComm *6*, 437–443.

Gazdik, M., Jarman, K.E., O'Neill, M.T., Hodder, A.N., Lowes, K.N., Jousset Sabroux, H., Cowman, A.F., Boddey, J.A., and Sleebs, B.E. (2016). Exploration of the P3 region of PEXEL peptidomimetics leads to a potent inhibitor of the *Plasmodium* protease, plasmepsin V. Bioorg. Med. Chem. *24*, 1993–2010.

Gero, A.M., and Wood, A.M. (1991). New nucleoside transport pathways induced in the host erythrocyte membrane of malaria and Babesia infected cells. Adv. Exp. Med. Biol. *309A*, 169–172.

Hamilton, W.L., Amato, R., van der Pluijm, R.W., Jacob, C.G., Quang, H.H., Thuy-Nhien, N.T., Hien, T.T., Hongvanthong, B., Chindavongsa, K., Mayxay, M., et al. (2019). Evolution and expansion of multidrug-resistant malaria in southeast Asia: a genomic epidemiology study. Lancet Infect. Dis. *19*, 943–951.

Hawking, F., Wilson, M.E., and Gammage, K. (1971). Evidence for cyclic development and short-lived maturity in the gametocytes of *Plasmodium falciparum*. Trans. R. Soc. Trop. Med. Hyg. *65*, 549–559.

Hermand, P., Cicéron, L., Pionneau, C., Vaquero, C., Combadière, C., and Deterre, P. (2016). *Plasmodium falciparum* proteins involved in cytoadherence of infected erythrocytes to chemokine CX3CL1. Sci. Rep. *6*, 33786.

Hiller, N.L., Bhattacharjee, S., van Ooij, C., Liolios, K., Harrison, T., Lopez-Estraño, C., and Haldar, K. (2004). A host-targeting signal in virulence proteins reveals a secretome in malarial infection. Science *306*, 1934–1937.

Hliscs, M., Millet, C., Dixon, M.W., Siden-Kiamos, I., McMillan, P., and Tilley, L. (2015). Organization and function of an actin cytoskeleton in *Plasmodium falciparum* gametocytes. Cell. Microbiol. *17*, 207–225.

Ho, C.M., Beck, J.R., Lai, M., Cui, Y., Goldberg, D.E., Egea, P.F., and Zhou, Z.H. (2018). Malaria parasite translocon structure and mechanism of effector export. Nature *561*, 70–75.

Hodder, A.N., Sleebs, B.E., Czabotar, P.E., Gazdik, M., Xu, Y., O'Neill, M.T., Lopaticki, S., Nebl, T., Triglia, T., Smith, B.J., et al. (2015). Structural basis for plasmepsin V inhibition that blocks export of malaria proteins to human erythrocytes. Nat. Struct. Mol. Biol. *22*, 590–596.

Ikadai, H., Shaw Saliba, K., Kanzok, S.M., McLean, K.J., Tanaka, T.Q., Cao, J., Williamson, K.C., and Jacobs-Lorena, M. (2013). Transposon mutagenesis identifies genes essential for *Plasmodium falciparum* gametocytogenesis. Proc. Natl. Acad. Sci. USA *110*, E1676–E1684.

Joice, R., Nilsson, S.K., Montgomery, J., Dankwa, S., Egan, E., Morahan, B., Seydel, K.B., Bertuccini, L., Alano, P., Williamson, K.C., et al. (2014). *Plasmodium falciparum* transmission stages accumulate in the human bone marrow. Sci. Transl. Med. *6*, 244re5.

Kafsack, B.F., Rovira-Graells, N., Clark, T.G., Bancells, C., Crowley, V.M., Campino, S.G., Williams, A.E., Drought, L.G., Kwiatkowski, D.P., Baker, D.A., et al. (2014). A transcriptional switch underlies commitment to sexual development in malaria parasites. Nature *507*, 248–252.

Kirk, K., and Lehane, A.M. (2014). Membrane transport in the malaria parasite and its host erythrocyte. Biochem. J. *457*, 1–18.

Klemba, M., and Goldberg, D.E. (2005). Characterization of plasmepsin V, a membrane-bound aspartic protease homolog in the endoplasmic reticulum of *Plasmodium falciparum*. Mol. Biochem. Parasitol. *143*, 183–191.

Kraemer, S.M., and Smith, J.D. (2006). A family affair: var genes, PfEMP1 binding, and malaria disease. Curr. Opin. Microbiol. *9*, 374–380.

Lucantoni, L., Duffy, S., Adjalley, S.H., Fidock, D.A., and Avery, V.M. (2013). Identification of MMV malaria box inhibitors of *plasmodium falciparum* early-stage gametocytes using a luciferase-based high-throughput assay. Antimicrob. Agents Chemother. *57*, 6050–6062.

Lucantoni, L., Fidock, D.A., and Avery, V.M. (2016). Luciferase-Based, High-Throughput Assay for Screening and Profiling Transmission-Blocking Compounds against *Plasmodium falciparum* Gametocytes. Antimicrob. Agents Chemother. *60*, 2097–2107.

Maier, A.G., Rug, M., O'Neill, M.T., Beeson, J.G., Marti, M., Reeder, J., and Cowman, A.F. (2007). Skeleton-binding protein 1 functions at the parasitophorous vacuole membrane to traffic PfEMP1 to the *Plasmodium falciparum*-infected erythrocyte surface. Blood *109*, 1289–1297.

Maier, A.G., Rug, M., O'Neill, M.T., Brown, M., Chakravorty, S., Szestak, T., Chesson, J., Wu, Y., Hughes, K., Coppel, R.L., et al. (2008). Exported proteins required for virulence and rigidity of *Plasmodium falciparum*-infected human erythrocytes. Cell *134*, 48–61.

Marapana, D.S., Dagley, L.F., Sandow, J.J., Nebl, T., Triglia, T., Pasternak, M., Dickerman, B.K., Crabb, B.S., Gilson, P.R., Webb, A.I., et al. (2018). Plasmepsin V cleaves malaria effector proteins in a distinct endoplasmic reticulum translocation interactome for export to the erythrocyte. Nat. Microbiol. *3*, 1010–1022.

Marti, M., Good, R.T., Rug, M., Knuepfer, E., and Cowman, A.F. (2004). Targeting malaria virulence and remodeling proteins to the host erythrocyte. Science *306*, 1930–1933.

Nguyen, W., Hodder, A.N., de Lezongard, R.B., Czabotar, P.E., Jarman, K.E., O'Neill, M.T., Thompson, J.K., Jousset Sabroux, H., Cowman, A.F., Boddey, J.A., and Sleebs, B.E. (2018). Enhanced antimalarial activity of plasmepsin V inhibitors by modification of the P_2 position of PEXEL peptidomimetics. Eur. J. Med. Chem. *154*, 182–198.

Obaldia, N., 3rd, Meibalan, E., Sa, J.M., Ma, S., Clark, M.A., Mejia, P., Moraes Barros, R.R., Otero, W., Ferreira, M.U., Mitchell, J.R., et al. (2018). Bone Marrow Is a Major Parasite Reservoir in *Plasmodium vivax* Infection. MBio *9*, e00625-18.

Pelle, K.G., Oh, K., Buchholz, K., Narasimhan, V., Joice, R., Milner, D.A., Brancucci, N.M., Ma, S., Voss, T.S., Ketman, K., et al. (2015). Transcriptional profiling defines dynamics of parasite tissue sequestration during malaria infection. Genome Med. *7*, 19.

Ponnudurai, T., Leeuwenberg, A.D., and Meuwissen, J.H. (1981). Chloroquine sensitivity of isolates of *Plasmodium falciparum* adapted to *in vitro* culture. Trop. Geogr. Med. *33*, 50–54.

Prommana, P., Uthaipibull, C., Wongsombat, C., Kamchonwongpaisan, S., Yuthavong, Y., Knuepfer, E., Holder, A.A., and Shaw, P.J. (2013). Inducible knockdown of *Plasmodium* gene expression using the *glmS* ribozyme. PLoS One *8*, e73783.

Ruecker, A., Mathias, D.K., Straschil, U., Churcher, T.S., Dinglasan, R.R., Leroy, D., Sinden, R.E., and Delves, M.J. (2014). A male and female gametocyte functional viability assay to identify biologically relevant malaria transmission-blocking drugs. Antimicrob. Agents Chemother. *58*, 7292–7302.

Rug, M., Prescott, S.W., Fernandez, K.M., Cooke, B.M., and Cowman, A.F. (2006). The role of KAHRP domains in knob formation and cytoadherence of *P. falciparum*-infected human erythrocytes. Blood *108*, 370–378.

Russo, I., Babbitt, S., Muralidharan, V., Butler, T., Oksman, A., and Goldberg, D.E. (2010). Plasmepsin V licenses *Plasmodium* proteins for export into the host erythrocyte. Nature *463*, 632–636.

Saliba, K.S., and Jacobs-Lorena, M. (2013). Production of *Plasmodium falciparum* gametocytes in vitro. Methods Mol. Biol. *923*, 17–25.

Sargeant, T.J., Marti, M., Caler, E., Carlton, J.M., Simpson, K., Speed, T.P., and Cowman, A.F. (2006). Lineage-specific expansion of proteins exported to erythrocytes in malaria parasites. Genome Biol. *7*, R12.

Silvestrini, F., Lasonder, E., Olivieri, A., Camarda, G., van Schaijk, B., Sanchez, M., Younis Younis, S., Sauerwein, R., and Alano, P. (2010). Protein export marks the early phase of gametocytogenesis of the human malaria parasite *Plasmodium falciparum*. Mol. Cell. Proteomics *9*, 1437–1448.

Sinden, R.E. (2017). Developing transmission-blocking strategies for malaria control. PLoS Pathog. *13*, e1006336.

Sinha, A., Hughes, K.R., Modrzynska, K.K., Otto, T.D., Pfander, C., Dickens, N.J., Religa, A.A., Bushell, E., Graham, A.L., Cameron, R., et al. (2014). A cascade of DNA-binding proteins for sexual commitment and development in *Plasmodium*. Nature *507*, 253–257.

Sleebs, B.E., Lopaticki, S., Marapana, D.S., O'Neill, M.T., Rajasekaran, P., Gazdik, M., Günther, S., Whitehead, L.W., Lowes, K.N., Barfod, L., et al. (2014a). Inhibition of Plasmepsin V activity demonstrates its essential role in protein export, PfEMP1 display, and survival of malaria parasites. PLoS Biol. *12*, e1001897.

Sleebs, B.E., Gazdik, M., O'Neill, M.T., Rajasekaran, P., Lopaticki, S., Lackovic, K., Lowes, K., Smith, B.J., Cowman, A.F., and Boddey, J.A. (2014b). Transition state mimetics of the Plasmodium export element are potent inhibitors of Plasmepsin V from *P. falciparum* and *P. vivax*. J. Med. Chem. *57*, 7644–7662.

Spielmann, T., and Gilberger, T.W. (2015). Critical Steps in Protein Export of Plasmodium falciparum Blood Stages. Trends Parasitol. *31*, 514–525.

Srivastava, A., Philip, N., Hughes, K.R., Georgiou, K., MacRae, J.I., Barrett, M.P., Creek, D.J., McConville, M.J., and Waters, A.P. (2016). Stage-Specific Changes in *Plasmodium* Metabolism Required for Differentiation and Adaptation to Different Host and Vector Environments. PLoS Pathog. *12*, e1006094.

Staines, H.M., Rae, C., and Kirk, K. (2000). Increased permeability of the malaria-infected erythrocyte to organic cations. Biochim. Biophys. Acta *1463*, 88–98.

Tibúrcio, M., Silvestrini, F., Bertuccini, L., Sander, A.F., Turner, L., Lavstsen, T., and Alano, P. (2012). Early gametocytes of the malaria parasite *Plasmodium falciparum* specifically remodel the adhesive properties of infected erythrocyte surface. Cell. Microbiol. *15*, 647–659.

Tibúrcio, M., Dixon, M.W., Looker, O., Younis, S.Y., Tilley, L., and Alano, P. (2015). Specific expression and export of the *Plasmodium falciparum* Gametocyte EXported Protein-5 marks the gametocyte ring stage. Malar. J. *14*, 334.

Triglia, T., Tham, W.H., Hodder, A., and Cowman, A.F. (2009). Reticulocyte binding protein homologues are key adhesins during erythrocyte invasion by *Plasmodium falciparum*. Cell. Microbiol. *11*, 1671–1687.

van der Pluijm, R.W., Imwong, M., Chau, N.H., Hoa, N.T., Thuy-Nhien, N.T., Thanh, N.V., Jittamala, P., Hanboonkunupakarn, B., Chutasmit, K., Saelow, C., et al. (2019). Determinants of dihydroartemisinin-piperaquine treatment failure in *Plasmodium falciparum* malaria in Cambodia, Thailand, and Vietnam: a prospective clinical, pharmacological, and genetic study. Lancet Infect. Dis. *19*, 952–961.

Waterkeyn, J.G., Wickham, M.E., Davern, K.M., Cooke, B.M., Coppel, R.L., Reeder, J.C., Culvenor, J.G., Waller, R.F., and Cowman, A.F. (2000). Targeted mutagenesis of *Plasmodium falciparum* erythrocyte membrane protein 3 (PfEMP3) disrupts cytoadherence of malaria-infected red blood cells. EMBO J. *19*, 2813–2823.

Weiss, D.J., Lucas, T.C.D., Nguyen, M., Nandi, A.K., Bisanzio, D., Battle, K.E., Cameron, E., Twohig, K.A., Pfeffer, D.A., Rozier, J.A., et al. (2019). Mapping the global prevalence, incidence, and mortality of *Plasmodium falciparum*, 2000-17: a spatial and temporal modelling study. Lancet *394*, P322–P331.

Werling, K., Shaw, W.R., Itoe, M.A., Westervelt, K.A., Marcenac, P., Paton, D.G., Peng, D., Singh, N., Smidler, A.L., South, A., et al. (2019). Steroid Hormone Function Controls Non-competitive Plasmodium Development in Anopheles. Cell *177*, 315–325.e4.

White, N.J. (2013). Primaquine to prevent transmission of falciparum malaria. Lancet Infect. Dis. *13*, 175–181.

STAR★METHODS

KEY RESOURCES TABLE

REAGENT or RESOURCE	SOURCE	IDENTIFIER
Antibodies		
Rabbit polyclonal anti-PMV	In house	Sleebs et al., 2014a
Mouse monoclonal anti-PMV	Daniel Goldberg	Klemba and Goldberg, 2005
Rabbit polyclonal anti-Aldolase	In house	Baum et al., 2006
Rabbit polyclonal anti-GAP45	In house	Baum et al., 2006
Mouse monoclonal anti-EXP2	In house	de Koning-Ward et al., 2009
Mouse monoclonal anti-SBP1	In house	Maier et al., 2007
Rabbit polyclonal anti-KAHRP	In house	Rug et al., 2006
Rabbit polyclonal anti-PfEMP3	In house	Waterkeyn et al., 2000
Rabbit polyclonal anti-GEXP07	In house	Sleebs et al., 2014a
Rabbit polyclonal anti-ATS	In house	Maier et al., 2007
Rat monoclonal 3F10 anti-HA	Roche	Cat# 11867423001, RRID: AB_390918
Rat anti-GFP agarose	MBL International	D153-8, RRID: AB_591815
Critical Instruments		
Delta Vision Elite microscope	GE Life Sciences	N/A
JEM 2010HC transmission electron microscope	JEOL	N/A
Experimental Models: Cells/Organisms/Strains		
Human O^+ erythrocytes	Melbourne Red Cross	N/A
Plasmodium falciparum CS2	Stephen Rogerson	Cooke et al., 1996
P. falciparum CS2 GEXP10-HA	This study	N/A
P. falciparum CS2 Δ*GEXP10*	This study	N/A
P. falciparum NF54	Walter Reed Army Institute of Research	Ponnudurai et al., 1981
P. falciparum $NF54^{Pfs16}$	David Fidock	Adjalley et al., 2011
P. falciparum NF54 GEXP10-GFP	This study	N/A
P. falciparum 3D7 GEXP05-GFP	Matthew Dixon	Tibúrcio et al., 2015
Anopheles stephensi	Johns Hopkins University	N/A
Reagents		
RPMI 1640 medium	GIBCO	Cat# 23400021
Albumax	Thermo Fisher Scientific	Cat# 11021029
Triton X-100	Sigma-Aldrich	Cat# T8787
Equinatoxin II	Leanne Tilley	Anderluh et al., 1996
Trypsin TPCK treated	Worthington USA	Cat# LS003740
Soybean Trypsin inhibitor	Worthington USA	Cat# LS003570
WEHI-916	In house	Sleebs et al., 2014a
WEHI-024	In house	Sleebs et al., 2014a
WEHI-025	In house	Sleebs et al., 2014a
WEHI-842	In house	Hodder et al., 2015
Software and Algorithms		
PlasmoDB	https://plasmodb.org/plasmo/	Bahl et al., 2002
SoftWorx	GE Life Sciences	N/A
FIJI	ImageJ	https://imagej.net/Fiji
Prism 7	GraphPad	https://www.graphpad.com/scientific-software/prism/

LEAD CONTACT AND MATERIALS AVAILABILITY

Further information and requests for resources and reagents should be directed to and will be fulfilled by the Lead Contact, Justin Boddey (boddey@wehi.edu.au). Reagents generated in this study are available from the Lead Contact with a completed Materials Transfer Agreement.

EXPERIMENTAL MODEL AND SUBJECT DETAILS

Culture Conditions for Parasite Maintenance

P. falciparum 3D7, CS2 and NF54 asexual-stages were maintained in human type O-positive erythrocytes (Australian Red Cross) in RPMI-HEPES supplemented with 10% heat-inactivated human serum (Australian Red Cross), at 37°C. Gametocytes for transmission to mosquitoes were generated using the "crash" method (Saliba and Jacobs-Lorena, 2013) using daily media changes. The GFP-luciferase line ($NF54^{Pfs16}$) (Adjalley et al., 2011), was maintained in human type O-positive erythrocytes (Australian Red Cross) in RPMI-HEPES supplemented with 5% AB human male serum (Sigma), 2.5 mg/ml Albumax II and 0.37 mM hypoxanthine, at 37°C, 90% N_2, 5% CO_2, 5% O_2 Gametocyte inductions for gametocytogenesis inhibition assays were performed using an established method (Duffy et al., 2016).

P. falciparum Gametocyte EC_{50} Determination

Gametocytes, at various stages of development, were exposed for 48 hours or 72 hours to the experimental compound in 384-well microtiter plates for luciferase (Optiplate, PerkinElmer) or imaging (CellCarrier, PerkinElmer). Compounds were tested in full dose-response, using three concentrations per log dose. Puromycin (5 μM) and DMSO (0.4%) were used as positive and negative controls, respectively. All microplate wells contained the same final DMSO concentration (0.4%). Plates were incubated with compounds at 90% N_2, 5% CO_2, 5% O_2. After incubation, the plates were read as described previously using a luciferase (Lucantoni et al., 2013, 2016) or imaging (Duffy and Avery, 2013) readout. Raw data was normalized using the respective in-plate positive and negative control values, to obtain % inhibition data.

Inhibition of Gametocyte Development

Synchronous NF54 were diluted to 0.6% parasitemia at 4% hematocrit, in a final volume of 10 mL and transferred to a 90 × 14mm Petri dish. RPMI-HEPES supplemented with 10% heat-inactivated O+ human serum media was used for maintenance of cultures. On days 1-3, 60% of the total volume was exchanged for fresh media. On day 4, 60% of the media was removed and the total volume was increased by 125%. On day 5, 60% of the total volume was exchanged for fresh media. On day 6 the ring stages (committed rings) of the infected RBCs were purified by magnetic separation using a Macs column (Miltenyi Biotech). Briefly trophozoites, schizonts and stage II-V gametocytes were column-retained and committed rings and uninfected RBCs were captured in the flow through. Flow through material was made up to a final volume of 24 mL and transferred to a 6-well plate as 4mL aliquots, supplemented with 50mM *N*-acetylglucosamine (NAG) and appropriate concentrations of WEHI-842 (solubilised in DMSO), or DMSO vehicle. 60% of the media (+NAG for first 3 days only), with appropriate concentrations of WEHI-842, or vehicle was exchanged daily for 12 days. Giemsa-stained blood smears were taken regularly over a period of 12 days post column purification for each condition. Giemsa stained smears were imaged using a Zeiss LiveCell AxioObserver at 100x magnification, as series of 64 or 100 tiles. At least 2 sets of 64 or 100 random tiles were counted (corresponding to > 2000 Red blood cells) for each condition.

P. falciparum Mosquito Infection and Analysis

Gametocyte cultures were spun at 2200 *g* for 5 min at 37°C, supernatant removed and resuspended in heat inactivated human serum at a ratio of 1:1 erythrocytes to serum. When > 0.3%, gametocytaemia was normalized to 0.3% with uninfected RBCs. Gametocyte containing bloodmeals were fed by standard membrane feeding assay to ~4 day old *Anopheles stephensi* mosquitoes (obtained from Johns Hopkins University). Unfed mosquitoes were removed post feed and mosquitoes maintained on 10% glucose/dextrose at 26°C and 80% humidity. Seven days post bloodmeal, mosquito midguts were dissected, stained with 0.1% mercurochrome and visualized under 100x magnification (Armistead et al., 2018). Prevalence of infection was determined by counting the number of mosquitoes with at least one oocyst from the total number of mosquitoes per group (Werling et al., 2019).

Ethics Statement

All work with human erythrocytes was approved by the Human Ethics Research Committees of the Walter and Eliza Hall Institute of Medical Research and the Griffith University Institute Biosafety Committee.

METHOD DETAILS

Transgenic Parasites

P. falciparum 3D7 parasites expressing GEXP05-GFP (PlasmoDB: PF3D7_0936600) were generated previously (Tibúrcio et al., 2015). A gametocyte stage-specific plasmid was constructed by amplifying the 5′ UTR of the gametocyte gene *Pfs16*

(PlasmoDB: PF3D7_0406200) from *P. falciparum* NF54 gDNA with the primers 5′-actgcggccgccaatatgaatttatagagcaaa-3′ and 5′-gatctcgaggttgaagaaagtataaatagaaaaatgg-3′ containing *Not*I and *Xho*I sites, respectively (restriction sites are underlined in the primer sequence). The *Pfs16* promoter was cloned into pGlux.1 (Boddey et al., 2009). DNA encoding GEXP10 (PlasmoDB: PF3D7_0112800) was cloned into pGlux.1 containing the *Pfs16* promoter with primers 5′-gatctcgagatgaacatttatattag gacc-3′ and 5′-gatcccgggttgaaaatgtaatatttgtc-3′ containing *Xho*I and XmaI sites, respectively. Purified plasmid DNA (100 μg, Life Technologies) was transfected into *P. falciparum* NF54 and stable transfectants were selected as described previously (Boddey et al., 2009).

To HA-tag GEXP10, the 3′ of the GEXP10 locus was amplified from *P. falciparum* 3D7 gDNA using primers 5′-atcagatctttgaaaatg taatatttgtc-3′ and 5′-atcctgcagggacaaatattacattttcaa-3′. The amplicon was cloned into pHA3 (Triglia et al., 2009) via BglII and PstI. Purified plasmid DNA (100 μg, Life Technologies) was transfected into *P. falciparum* 3D7 and stable transfectants were selected as described previously (Boddey et al., 2010). Integration of the cassette was confirmed by immunoblot with anti-HA antibodies.

To disrupt the *P. falciparum* GEXP10 locus, 5′ and 3′ flanks were amplified from *P. falciparum* CS2 gDNA using primers aw594 5′-atccgcggtggtacataaccaaggaaataaggg-3′ and aw565 5′-gatactagtggtaactacctgaacaattcaggc for the 5′ flank and aw596 5′-atcgaattctatgattcaaatttgttgaaaagtg-3′ and aw597 5′-gatcctaggcaatgtggatatcacaaaatgaaag-3′ for the 3′ flank. Amplicons were cloned into pCC1 via *Sac*II/*Spe*I (5′ flank) and EcorRI/AvrII (3′ flank) to generate the knockout construct. Purified plasmid DNA (100 μg, Life Technologies) was transfected into *P. falciparum* CS2 and stable transfectants were selected as described previously (Duraisingh et al., 2002). Transfected lines were cloned by limiting dilution and the expected genotypic disruption of the PfGEXP10 locus was confirmed by diagnostic PCR screens.

Microscopy

Highly synchronous asexual and sexual stages were sampled at ring stage and, for gametocytes, throughout gametocytogenesis. Cells were fixed in methanol and stained with Giemsa or fixed in 4% v/v paraformaldehyde (PFA, Sigma-Aldrich), 0.0075% v/v glutaraldehyde and probed with primary antibodies: rabbit anti-PMV 1:500 (Sleebs et al., 2014a), mouse anti-PMV 1:25 (MRA-815A from MR4) (Klemba and Goldberg, 2005), rabbit anti-GAP45 1:200 (Baum et al., 2006), rat anti-HA 1:50 (Roche 3F10), mouse anti-EXP2 (1:200) (de Koning-Ward et al., 2009), mouse anti-SBP1 1:500 (Maier et al., 2007), rabbit anti-KAHRP (1:500) (Rug et al., 2006), rabbit anti-PfEMP3 1:500 (Waterkeyn et al., 2000), rabbit anti-GEXP07 (Hyp8) (Sleebs et al., 2014a) all in 3% BSA/PBS. Secondary antibodies were goat anti-rabbit 594, or donkey anti-rat 488, or goat anti-mouse 594 1:1000 (Invitrogen) in 3% BSA/PBS. DNA was stained with 4', 6-diamidino-2pheynlindole, dihydrochloride (DAPI) at 0.2 μg/ml. Samples were viewed on a Delta vision Elite microscope and images collected with a Coolsnap HQ2 CCD camera through an Olympus 1006 UPlanSApo NA1.4 objective with SoftWorx software. Images were assembled with ImageJ Fiji 1.47d and Adobe Photoshop CS6 v13.0 x64.

For immunoelectron microscopy, parasite infected erythrocytes were fixed with 1% glutaraldehyde in RPMI-HEPES (pH 7.2) on ice for 1 h, washed, and transferred into agarose blocks, which were dehydrated and embedded in LR Gold resin. The samples were infiltrated with a graded series of HM20 low-temperature resin in acetone, consisting of 25% resin (8 h), 50% resin (overnight), 75% resin (8 h), and 100% resin (overnight). The infiltrated samples were placed in a fresh change of 100% resin in gelatin capsules, polymerized under UV light for 48 h at −50°C, and brought to room temperature at 6°C per h. The soft sample blocks were hardened under UV light for a further 24 h at room temperature. Thin sections were prepared and incubated with the rat anti-HA antibodies (see above), followed by 10-nm-diameter gold-labeled anti-rat IgG. Sections were poststained with uranyl acetate and lead citrate to enhance contrast before examination in a JEOL JEM 2010HC transmission electron microscope.

Quantification of GEXP10 Export

Highly synchronous parasites were obtained by incubation of erythrocytes with viable sexual stage merozoites for 15 min (Boyle et al., 2010). Gametorings were treated with DMSO, 20 μM WEHI-842 or WEHI-024 18-20 hr post invasion for 4 hr. Cells were fixed in 4% v/v paraformaldehyde (PFA, Sigma-Aldrich), 0.0075% v/v glutaraldehyde to fix native GFP, permeabilized in 0.1% Triton X-100 for 10 min, washed thrice in PBS and probed with primary mouse anti-EXP2 (1:200) (de Koning-Ward et al., 2009) and Alexa Fluor 594-conjugated secondary antibodies (Molecular Probes; 1:1,000). DNA was stained with DAPI as above. Samples were viewed on a Zeiss LiveCell AxioObserver under 1000x magnification. Over 30 Z stacks per condition were imaged using the same exposure settings to allow quantitative analysis between groups. Exported and non-exported GFP intensity was measured as described previously (Sleebs et al., 2014a). Ratios of the average intensity measurements of GFP inside the parasite and PV (inside EXP2) versus exported to the erythrocyte (outside EXP2) were determined.

Immunoblotting, Membrane Topology and PfEMP1 Surface Display

For GEXP10-HA expression, parasite cultures were tightly synchronized by 5% sorbitol treatments 16 h apart and cultured to 5% parasitemia. Parasites were sampled at 8 h intervals post invasion and separated through 4%–12% Bis-Tris polyacrylamide gels (Invitrogen) by SDS-PAGE and transferred to nitrocellulose membranes that were probed with rabbit anti-PMV (1:5000) (Sleebs et al., 2014a), rat anti-HA 1:2500 (Roche, 3F10), rabbit anti-aldolase 1:1000 (Baum et al., 2006), rabbit anti-ATS 1:500 (Maier et al., 2007) antibodies followed by horseradish peroxidase-conjugated secondary antibodies (1:1000 (rat) and 1:4000 (rabbit); Cell Signaling Technology) and developed with enhanced chemiluminescence reagent (Amersham).

For topology assessment, asynchronous cultures were incubated with equinatoxin II (10 mg), 0.1% Saponin or 0.1% Triton X-100 in PBS with increasing concentrations of Trypsin (0, 10 and 25 μg/mL at RT for 30 min), followed by immunoblotting analysis as described above.

For assessment of PfEMP1 display on the infected erythrocyte surface, infected cells were incubated at room temperature for 1 h with 1 mg/ml Trypsin (Worthington USA), 1 mg/ml Trypsin with 1X soybean Trypsin inhibitor (Worthington USA), or in the absence of Trypsin as described previously (Maier et al., 2007), followed by immunoblotting as described above using anti-ATS antibodies.

Protein Radiolabelling, Pulse-Chase and Densitometry

Whole parasite proteins were radiolabelled by culturing magnet purified stage II gametocytes expressing GEXP05-GFP and GEXP10-GFP in the presence or absence of PMV inhibitor for 150 min at 37°C before labeling commenced. Gametocytes were washed after 150 min in the presence or absence of PMV inhibitor with Met/Cys-free medium and cultured for 30 min at 37°C. Gametocytes were radiolabelled with the addition of 800 μCi/ml 35-S-Met/Cys (Perkin/Elmer) to the medium for 10 min. Pellets were snap frozen in ethanol/dry ice bath and stored at −80°C. Frozen samples were solubilized in 25 mM Tris pH 8.0, 150 mM NaCl, 2 mM EDTA, 1% Triton X-100 in PBS with protease inhibitor cocktail (Roche) and immunopurified with α-GFP agarose (MBL) at 4°C for 1 h and proteins were resolved by SDS-PAGE, visualized by autoradiography (6-d exposure), and quantified using a GS-800 Calibrated Densitometer (Bio-Rad).

QUANTIFICATION AND STATISTICAL ANALYSIS

GraphPad Prism 7 software (GraphPad) was used to perform statistical tests and to determine sample size for experiments based on anticipated effect sizes. EC_{50} values were obtained from normalized inhibition data via a 4-parameter logistic curve fitting function in GraphPad Prism. Oocyst intensities were compared using Kruskal-Wallis test with Dunn's correction and mosquito infection prevalence was compared using Chi-square test. Non-parametric data was log-transformed for statistical analysis, or when this failed to normalize the data, Mann-Whitney tests were used. Error bars and biological repeats are indicated in the figure legends.

DATA AND CODE AVAILABILITY

Not applicable.